CHEMICAL ENGINEERING TRANSACTIONS
VOL. 60, 2017
A publication of AIDIC
The Italian Association of Chemical Engineering
Online at www.aidic.it/cet
Guest Editors: Luca Di Palma, Elisabetta Petrucci, Marco Stoller

ISBN978-88-95608- 50-1; **ISSN** 2283-9216
DOI: 10.3303/CET1760007

Elaboration and Enhanced Activity of the Mixed Oxide $Zr_xTi_{1-x}O_2$ Nano-photocatalyst

Khley Cheng, Khay Chhor, Andrei Kanaev

Laboratoire des Sciences des Procédés et des Matériaux, CNRS, Université Paris 13, Sorbonne Paris Cité, 93430 Villetaneuse, France
andrei.kanaev@lspm.cnrs.fr

The photocatalysis activity of mixed nanocomposite $Zr_xTi_{1-x}O_2$ catalyst was studied. The catalysts with x=0, 0.1 and 0.2 were prepared via sol-gel method in a reactor with rapid micromixing using titanium tetra-isopropoxide and zirconium tetra-propoxide precursors and n-propanol solvent. The colloids were coated on cleaned borosilicate beads and treated at temperatures in the range between 400 and 600 °C to achieve crystalline anatase phase. The prepared materials were characterized by ICP-OES, BET, TDA and optical absorption measurements. The photocatalytic experiments were carried out in a continuous-flow fixed bed reactor on the gaseous ethylene decomposing. The photocatalytic activity of the prepared material was depended on the elemental compositions and calcination temperature. The enhanced activity, 50% higher compared to pure anatase TiO_2, was obtained in the material containing 10 mol% Zr and thermally treated at 500 °C.

1. Introduction

The applications by TiO_2 in photocatalysis have been known for few decades, because it is efficient, not expensive and non-toxic material showing long-time stability in the photocatalytic process (Hashimoto et al., 2005). The photocatalytic decomposition of pollutants in gas and liquid phases is related to the generation of a hole in valence band and electron in the conduction band when the light is applied on this semiconductor material. The activity of pure TiO_2 can be still improved by doping and/or mixing with metals or other metal oxides (Michael et al, 2014).

Many studies have been devoted to the preparation of the mixed ZrO_2-TiO_2 catalyst. The successful preparation is related to the most homogeneous mixing of the two solids on the molecular level and adequate annealing. Between different preparation techniques, co-precipitation and sol-gel methods have deserved a particular interest and were used more often than others (Reddy et al. 2007, Khan et at. 2015, Li et al. 2011). As a result of these studies, the ZrO_2-TiO_2 composite was found to be an interesting material for use as catalyst, supported catalyst and photocatalyst (Reddy et al. 2007). The mixed composite ZrO_2-TiO_2 photocatalyst has been used for the degradation of several organic compounds, such as trichloroethylene (Kyeong et al, 2004) and methylene blue (Mahdi et al, 2016). The composite photocatalyst showed some improvement in efficiency recently (Li et al. 2015, Wu et al. 2009). In the same, the nanoscale homogeneity has not been addresses in these studies and compositional and structural homogeneity of the ZrO_2-TiO_2 photocatalyst was not confirmed.

Recently, monodispesity and high homogeneity $Zr_xTi_{1-x}O_2$ nanoparticles of variable elemental composition $0 \le x \le 1$ were realized in our team by using rapid micromxing reactor (Cheng et al. 2017). The mixing on a molecular level takes place at the fluids contact in very short time of several milliseconds, before the reactions between the precursors and water in solvent begin leading to the solid phase nucleation (Azouani et al, 2010).

In this present communication, we report on studies of the photocatalysis activity of the mixed metal oxides $Z_xTi_{1-x}O_2$ nanocomposite. The materials were prepared as stable monodispersed oxo-alkoxy colloidal nanoparticles of a controlled elemental composition, followed by their coating on the borosilicate glass beds and heat treatment. We show that the photocatalytic activity of the prepared material sensitively depends on

Please cite this article as: Cheng K., Chhor K., Kanaev A., 2017, Elaboration and enhanced activity of the mixed oxide zrxti1-xo2 nano-photocatalyst, Chemical Engineering Transactions, 60, 37-42 DOI: 10.3303/CET1760007

the elemental composition x and calcinations temperature T_c. The highest activity was found for the material with x=0.1 heat treated at 500 °C, which was 1.5 times higher than that of pure TiO_2.

2. Experimental

2.1 Photocatalyst preparation

The sol-gel reactor used for the nanoparticles synthesis has been previously described (Rivallin et al. 2002; Rivallin et al. 2005; Azouani et al. 2010). In short, two stock solutions containing (A) precursors of zirconium (IV) propoxide (70 wt%, Sigma-Aldrich) and titanium (IV) isopropoxide (98%, Sigma-Aldrich) in n-propanol (99.5%, Sigma-Aldrich) and (B) distilled and twice filtered water (syringe filter 0.1 µm porosity PALLs Acrodisc) in n-propanol were prepared in a LABstar glove box workstation (MBraun) in order to avoid any contamination with atmospheric humidity (H_2O vapour traces below 0.5 ppm). The total concentration of the precursors was $C_{pr}=C_{Ti}+C_{Zr}=0.292$ mol/l and the hydrolysis ratio $H=C_w/C_{pr}=1.25$, where C_w is water concentration. These solutions were transferred to the reactor reservoirs under nitrogen flow to prevent moisture and oxygen absorbed into solutions. The preparation and transfer time was around 25 min. The micromixing of the reacting solutions A and B was achieved by the injection in a static T mixer with exocentric input arms of 1 mm diameter and output tube of 2 mm diameter, by applying nitrogen gas pressure of 4 bar to the reactor reservoirs. The injecting fluids propagate through the T mixer with a speed of 10 m/s with the Reynold's number Re≈6000 maintained at the temperature of 20.0 °C with a thermo-cryostat Haake, DC10K15). The particle size was controlled with the DLS (dynamic light scattering) method using monomode optical fiber probe, 40 mW / 640 nm single-frequency laser Cube 640-40 Circular (Coherent) and 48 bits 288 channels photon correlator Photocor-PC2 (PhotoCor Instruments). The optimal operating regime of the sol-gel reactor corresponds to the Damköhler number Da≤1 that permits point-like reaction conditions and the smallest polydispersity of the produced nanoparticles. The reactor permits preparation of ~1 g of size-selected nanoparticles by injection lasted ~10 s.

The photocatalyst was prepared after the coating of colloidal nanoparticles on borosilicate glass beads followed by drying at 80°C overnight and heat treatment at temperatures in the range between 400 and 600°C for 4 hours. The beads were preliminary cleaned in concentrated sulfuric acid (95-98%), rinsed in distillated water and dried at 80 °C. The dried borosilicate beads were set in contact for 10 min with the colloidal solutions containing $Zr_xTi_{1-x}O_2$ nanoparticles, which react with the surface hydroxyls forming thin coating.

2.2 Characterization

The $Zr_xTi_{1-x}O_2$ nanopowders were characterized by differential thermal analysis DTA (SETARAM) under oxygen gas (1bar). The selected temperatures in Table 1 were used to calcinate photocatalytic powders and coatings. BET COULTER SA3100 was used to measure surface areas of the powder materials. To analyze the amount and real compositions on beads, the coated amorphous oxo-nanoparticles on beads were dissolved in concentrated nitric acid and stirring at 60 °C for 1 hour and then diluted with distilled water. These diluted solutions were analyzed by ICP-OES (iCAP 6000). The optical absorption of the $Z_xTi_{1-x}O_2$ photocatalyst was measured after the nanoparticles deposition of borosilicate glass plates using Jasco V-660 UV-visible spectrometer. For these measurements, the coatings of the colloidal nanoparticles on quart substrates were prepared by applying the prepared procedure of the borosilicate glass beads.

Table 1: The compositions and temperatures were selected to do calcinations

Compositions, x	0.0	0.1	0.2
$T_{calcinations}$, °C	410	500	600

2.3 Photocatalytic measurements

The photocatalytic experiments were conducted in a laboratory-made continuous gas flow fixed bed reactor (Benmami et al. 2005). The ethylene gas was used as a model pollutant at the concentration 120 ppm ethylene mixed with synthetic air at the flow rate 75 mL/min. The reactor tube of 6 mm diameter, transparent in UVA spectral above 320 nm, was filled with the photocatalyst is surrounded with six 8-W lamps emitting at 362±11 nm. The inlet (Cin) and outlet (Cout) ethylene concentrations were monitored by a gas chromatograph (Varian CP 3800) equipped with GC-FID detector and loops allowing the continuous injection mode. The reactor yield was calculated as $\eta(\%)=(1-Cout/Cin)100$. The stationary temperature of 45 °C (monitored with chromel/alumel thermocouple (T)) was established in the reactor during a short time of 3 min after the UVA lamp on.

3. Results and discussion

3.1 Photocatalyst characterization

To evaluate the amounts and compositions of the photocatalyst on borosilicate beads, the films were analyzed by ICP-OES. As Table 2 shows, the photocatalyst compositions after the synthesis conditions and ICP measurements are almost similar. This indicates no losses of the material (no Ti neither Zr) during the deposition process and confirms the homogeneous nucleus composition reported by Cheng at al. (2017).
The coating thickness is an important factor for the photoctalysis activity, since it determines the absorbance of the UVA lamp photons. The total amount of Ti and Zr of was measured for each photocatalyst composition coating and then converted to the coatings thickness. The results show that all prepared coatings were almost 10 nm thick, which is close to the two layers coverage by nanoparticles. There were not significant differences for each other (% SD ≈ 7%).

Table 2: Composition and thickness of photocatalysts coated on glass beads.

X , synthesis	Total of n_{Ti+Zr}, µmol	Thickness on beads, nm	X , ICP
beads	0.2	0.15	-
0.0	13.2	9.34	0.00
0.10	11.3	8.12	0.095
0.20	12.1	8.78	0.17

The crystallisation temperatures of the photocatalyst were obtained from DTA characterisation presented in Figure 1a. According to these measurements, the onset crystallisation temperature increased with the zirconium addition to titania from x=0.0 to 0.1 and 0.2 and constitute respectively 378, 462 and 573 °C. According to the DTA results, the heat treatment temperatures of the photocatalyst were chosen as depicted in Table 1.
The absorbance measurements of the coatings are shown in Figure 1b. To increase the contrast, the coatings prepared for these measurements were considerably thicker (~100 nm) compared to the photocatalytic ones (~10 nm). On the other hand, the extraction of absorption onset (and band gap energy) from these data was complicated by the interference effects. The analysis is under way. However, our results permit to conclude that the band gap energy of $Z_xTi_{1-x}O_2$ nanocomposite is not much dependent on its compositions for $0 \leq x \leq 0.2$ and is about that of the pure anatase TiO_2.

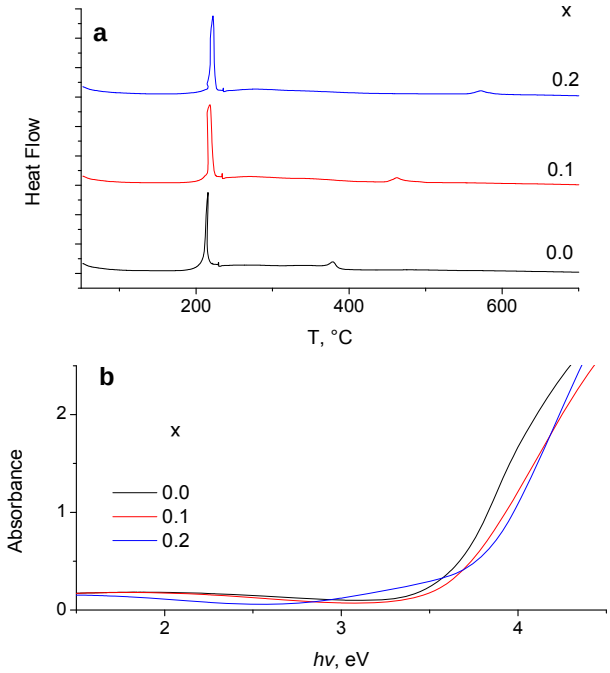

Figure 1: DTA measurements (a) and absorbance (b) of $Zr_xTi_{1-x}O_2$ photocatalyst coatings with x = 0.0, 0.1 and 0.2.

The x-ray diffraction measurements implemented on samples showed that the coatings conserved the anatase structure of TiO_2 fo relatively low Zr addition $x \leq 0.2$. For higher $x \geq 0.3$ the orthorhombic $Zr_xTi_{1-x}O_2$ phase appeared, which photocatalytic activity with the UVA illumination was negligible. The band gap energy of anatase TiO_2 seems not to be sensitive to the Zr addition unless other crystalline phases do not nucleate.
According to our DLS measurements, the nanoparticles size was sensitive to the elemental composition and smoothly increased from 3.0 to 3.7 nm at the composition change from x=0 to 0.2. Comparing with the measured thickness, one can conclude about 2-4 particles layers forming the coating in Table 2.
These results of BET measurements of the photocatalytic powders are shown in Figure 2. The specific areas of 25, 66 and 44 m^2/g were respectively obtained for x = 0.0, 0.1 and 0.2.

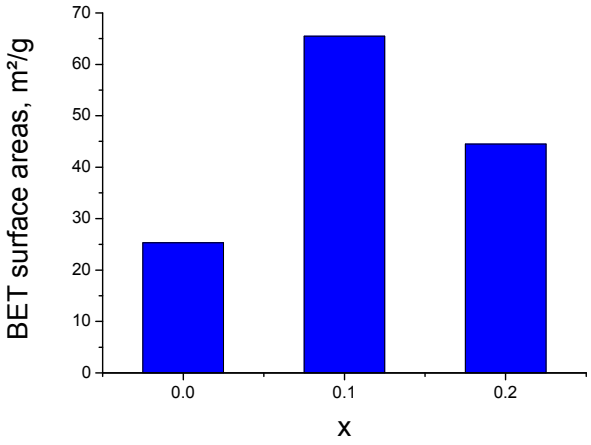

Figure 2: BET surface areas of different prepared $Z_xTi_{1-x}O_2$ photocatalyst.

3.2 Photocatalytic activity

The photocatalytic reactor yield of ethylene decomposition is shown in Figure 3. Two process cycles are shown: each begins with the label “on”, corresponding to the illumination of UVA lamps, and terminates with “off”. In the first cycle, the percentages of decomposing ethylene increased after the photocatalyst illumination reaching a stationary regime after about 25 min from the beginning of lamp illumination. The drop off of the photocatalytic activity is quasi-instantaneous when the lamps were turn off. In the second cycle, the activity was increased more rapidly (during several minutes) that corresponds to characteristic time of the UVA lamps intensity increase. The stationary yield of the reactor did not change with the number of cycles, which indicates the catalyst stability.

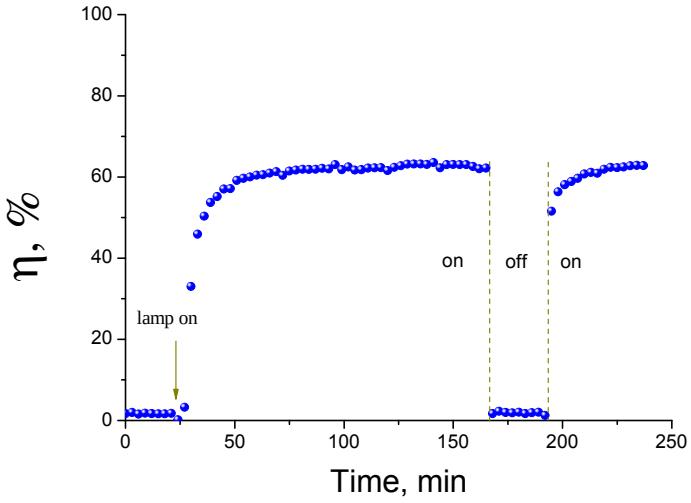

Figure 3: Ethylene conversion as function of time using $Zr_{0.1}Ti_{0.9}O_2$ *nanocoating calcinated at 500 °C (120 ppm ethylene under flow 75 mL/min).*

3.2.1 Influence of elemental compositions

To figure out the improved activity of the composite $Zr_xTi_{1-x}O_2$ photocatalyst, we performed the experiments of x = 0, 0.1 and 0.2 calcinated at temperatures depicted in Table 1. The stationary behaviour of the photocatalytic reactor are presented in Figure 4 with y-axis $\ln(C_{in}/C_{out})$, which is directly related to the reaction rate of the first order, which is general case of the ethylene decomposition. According to these results, the activity of the composite photocatalyst with x=0.1 was the highest: 50% higher better than that of pure anatase TiO_2. The activity decreased when larger amount of zirconium was added.

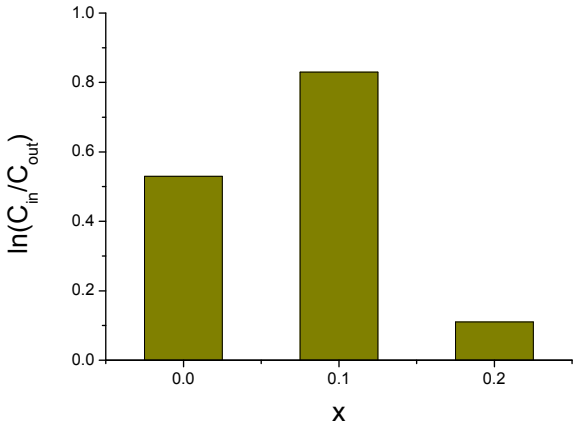

Figure 4: The dependence of photocalytic activity of $Zr_xTi_{1-x}O_2$ photocatalyst on elemental composition.

According to the absorbance measurements, the band gap shift cannot be the reason of the photocatalytic activity enhancement for x=0.1. The explanation of this effect seems to be the electron/hole transport and electron-hole recombination in the composite $Zr_xTi_{1-x}O_2$ semiconductor.

3.2.2 Influence of calcinations temperature

To do better investigation, we observed how effect of treatment temperatures on photocatalysis activity. The calcinations were very effective to the activity of photocatalyst. For the pure TiO_2, the photocatalysis activity was stable in different temperature treatments of the films from 400 to 500°C and less active when the temperature treatment was increased to 550°C. The different from pure TiO_2 activity, the composite $Zr_xTi_{1-x}O_2$ was strong or less active depending on temperature treatments. As shown in Figure 5, the activity of composition x=0.1 strongly increased with reached maximum at 500 °C when the treatment temperatures were increased from 400 °C. The degradation was less when the treatment was higher than 500 °C, which was similar to that found in our previous studies of nanostructured N-TiO_2 photocatalisst (Azouani et al., 2009).

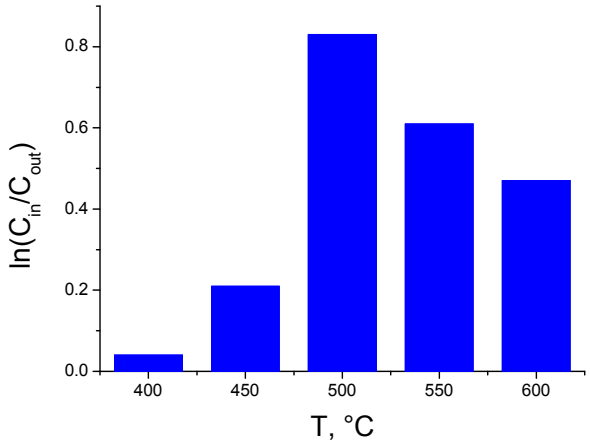

Figure 5: The dependence of photocalytic activity of $Zr_{0.1}Ti_{0.9}O_2$ photocatalyst on calcinations temperature.

The photocatalytic activity of $Zr_{0.1}Ti_{0.9}O_2$ expectantly increases with the temperature of heat treatment up to 500 °C due to the anatase crystallisation onset at 462 °C obtained from DTA measurements (Figure 1a). Apparently, the following decrease (T>500 °C) is not related to the anatase-rutile phase transition and we tentatively explain this behaviour by a decrease of the specific surface area of the photocatalyst.

4. Conclusions

The $Zr_xTi_{1-x}O_2$ photocatalysts (x = 0, 0.1 and 0.2) with highly homogeneous elemental and structural composition was succeeded prepared and the photocatalytic performance was studied on the gaseous ethylene decomposition in a continuous-flow fixed-bed reactor. The monodispersed $Zr_xTi_{1-x}O_2$ nanoparticles with the controlled elemental composition were nucleated in a sol-gel reactor with rapid (millisecond range of times) micromixing of the reacting fluids, followed by their chemical colloid deposition on borosilicate glass beads and heat treatment close to the phase transformation onset in the temperature range between 400 and 600°C. We show that the nucleus size (from 3.0 to 3.7 nm) and calcinations onset temperature (from 378 to 573 °C) increase with x, The $Zr_{0.1}Ti_{0.9}O_2$ photocatalysts showed the highest activity towards gaseous ethylene decomposition, which was 50% higher compared to that of pure anatase TiO_2.

Acknowledgments

ANR (Agence Nationale de la Recherche) and CGI (Commissariat à l'Investissement d'Avenir) are gratefully acknowledged for their financial support of this work through Labex SEAM (Science and Engineering for Advanced Materials and devices) ANR 11 LABX 086, ANR 11 IDEX 05 02. One of us (Khley Cheng) is grateful to the University of Uppsala under International Science Programme (ISP) for financial support of his PhD fellowship.

References

Azouani, R., Michau, A., Hassouni, K., Chhor, K., Bocquet, J. F., Vignes, J. L., Kanaev, A., 2010, Elaboration of pure and doped TiO_2 nanoparticles in sol-gel reactor with turbulent micromixing: Application to nanocoatings and photocatalysis, Chem. Eng. Res. Design, 88, 1123-1130.

Azouani, R., Tieng, S., Michau, A., Hassouni, H., Chhor, K., Bocquet, J. F., Vignes, J. L., Kanaev, A., 2009, Elaboration of doped and composite nano-TiO_2, Chem. Eng. Trans., 17, 981-986.

Benmami, M., Chhor, K., Kanaev, A. V., 2005, Supported nanometric titanium oxide sols as a new efficient photocatalyst, J. Phys. Chem. B, 109, 19766-19771.

Benmami, M., Chhor, K., Kanaev, A., 2005, Supported nanometric sols of titanium oxide for applications in photocatalysis, AIDIC Conf. Ser. Selected papers of IcheaP-7, 7, 29-38.

Cheng, K., Chhor, K., Brinza, O., Vrel, D., Kanaev, A. 2017, From nanoparticles to bulk crystalline solid: Nucleation, growth kinetics and crystallisation of mixed oxide $Zr_xTi_{1-x}O_2$ nanoparticles, 2017, submitted.

Hashimoto, K., Irie, H., Fujishima, A., 2005, TiO_2 photocatalysis: A historical overview and future prospects, Jap. J. Appl. Phys., 44, 8269-8285.

Khan, S., Kim J., Sotto, A., Van der Bruggen, B., 2015, Humic acid fouling in a submerged photocatalytic membrane reactor with binary TiO_2-ZrO_2 particles, J. Ind. Eng. Chem., 21, 779-786.

Kyeong Y. J., Seung B. P., 2004, Photoactivity of SiO_2/TiO_2 and ZrO_2/TiO_2 mixed oxides prepared by sol-gel method, Mater. Lett., 58, 2897-2900.

Li, K. T., Wang, C. K., Wang, I., Wang, C. M., 2011, Esterification of lactic acid over TiO_2-ZrO_2 catalysts, App. Catal. A : General, 392, 180-183.

Li, M., Li, X., Jiang, G., He, G., 2015, Hierarchically macro-mesoporous ZrO_2-TiO_2 composites with enhanced photocatalytic activity, Ceram. Int., 41, 5749-5757.

Mahdi B., Changiz D., Peyman T., Masoud B., 2016, Effect of duty cycle and electrolyte additive on photocatalytic performance of TiO_2-ZrO_2 composite layers prepared on CP Ti by micro arc oxidation method, Surf. Coat. Technol., 307, 554-564.

Michael D., Yiding L., Yadong Y., 2014, Composite titanium dioxide nanomaterials, Chem. Rev., 114, 9853-9889.

Rivallin, M., Zeghlache, A., Soloviev, A., Gaunand, A., Kanaev, A., 2002, Production of monodispersed nanometric sols of titanium oxide, Chem. Eng. Trans. 1, 969.

Reddy, B. M., Khan, A., 2007, Recent advances on TiO_2-ZrO_2 mixed oxides as catalysts and catalyst supports, Catal. Rev. 47, 257-296.

Rivallin, M., Benmami, M., Kanaev, A., Gaunand, A., 2005, Sol-gel reactor with rapid micromixing: modelling and measurements of titanium oxide nano-particles growth, Chem. Eng. Res. Design, 83, 67-74.

Wu, B., Yuan R., Fu X., 2009, Structural characterization and photocatalytic activity of hollow binary ZrO_2/TiO_2 oxide fibers, J. Solid State Chem., 182, 560-565.